Limnol. Oceanogr., 46(7), 2001, 1794–1802

A comparison of two N-irradiance interaction models of phytoplankton growth

Abstract—The N-photoacclimation interaction models of Geider et al. (GM) and Flynn et al. (FM) are compared by tuning them to data from a light-shift experiment for a diatom. Both the original model constructs have failings, GM in its N-assimilation component and FM in its photoacclimation component. However, both of these models can be modified readily to overcome these problems. In addition, hybrid models that use the N-assimilation component of FM and the photoacclimative component of GM work well. For situations where a model is required to simulate the interaction between a single N source and light, the use of the revised GM structure should be considered first. The revised FM is better suited for more complex environmental scenarios—for example where detailed simulations of ammonium-nitrate interactions are required. GM and FM are to be preferred over models that use a fixed Chl : C, because they may both be tuned directly to real chlorophyll *a* data in ecosystem simulators.

The interaction between nitrogen assimilation and irradiance is of considerable importance for growth of phytoplankton. The interaction involves the partitioning of the energy generated by photosynthesis among carbon assimilation, nitrogen assimilation, and biosynthesis. It also involves the feedback between photosynthetic energy conversion and carbon-nitrogen metabolism through the synthesis and turnover of chlorophyll *a*, together with the coupling/uncoupling of carbon assimilation and nitrogen assimilation through the build-up and consumption of energy storage reserves and intracellular nitrogen pools. There have been many models that have considered one or other of the potentially limiting factors (see Zonneveld 1998*a*) but few in which the interaction has been simulated in a fashion that could be deemed dynamic. Although Zonneveld (1998*b*) makes a case to formulate algal models on a cell basis, more frequently C is used as the ''currency'' because biochemistry operates at the level of substrate concentrations. C-based models are more general, do not need size structures, and are more convenient for inclusion within ecosystem models where the cycling of elements is of greatest concern. Models that explicitly include chlorophyll also provide a dynamic link between ocean optics and ocean biogeochemistry. This link will allow the extensive and growing database of satellite-derived estimates of surface ocean Chl *a* concentrations to be exploited in estimating phytoplankton nitrogen and carbon concentrations for comparison with models of upper ocean biogeochemistry that are often formulated in terms of N and/or C.

Here we present a comparison between the structures of the nitrogen-light colimitation models of Geider et al. (1996, 1997, 1998; referred to as GM), and the models of Flynn et al. (1997), Flynn and Fasham (1997), and Flynn and Flynn (1998; collectively referred to as FM). GM originated in an examination of photoacclimation of Chl *a* : C under nutrient-replete conditions (Geider et al. 1996), which was extended to include nitrogen assimilation (Geider et al. 1998). FM is derived from the ammonium-nitrate interaction model of Flynn et al. (1997), which was simplified to SHANIM by Flynn and Fasham (1997) and extended to include photoacclimation (Flynn and Flynn 1998; Flynn and Hipkin 1999). Both models depict N-light colimitation of algal growth as including photoacclimation with variable Chl : C rather than relying simply on fixed photosynthesis-irradiance (PE) curves.

For brevity, only equations pertinent to the discussion are given here. The names of parameters have been altered to be consistent with each other and with the latest model described by Flynn (2001). Full descriptions of the models are given in Web Appendix 1 at http://www.aslo.org/lo/toc/vol_46/issue_7/1794a1.pdf. The files to run the models with the software Powersim Constructor (Powersim AS, Isdalstø, Norway) are available from the corresponding author. Only those parameters and equations germane to this article are given here (in Tables 1 and 2).

Comparison of model structures—State variables: GM contains three state variables (for C, N, and Chl *a*, all expressed as g L^{-1} of water). It is essentially a dual nutrient (single N source plus light) quota-based model with growth dynamics controlled by N : C and Chl : C quotas. The model can be reconstructed readily with these quotas (rather than N L^{-1} and Chl *a* L^{-1}) as state variables. Temperature control may be introduced at various levels within GM (Geider et al. 1998), as it may within FM (Flynn 1999, in press).

Although GM considers a single N source, FM was specifically designed to handle details of the interaction between ammonium and nitrate. To do so, FM employs an additional state variable that describes an early product of N assimilation (named as glutamine; Flynn et al. 1997; Flynn and Fasham 1997). The original ammonium-nitrate interaction model (ANIM) of Flynn et al. (1997) also included state variables for internal inorganic N pools and for nitrate/nitrite reductase. FM is thus an ''internal pools'' model containing various feedback controls, describing C as g L^{-1}, with N, Ch l, and internal glutamine all expressed as C quotas.

Control of growth via N : C: Both models contain a quota-type control of photosynthesis, nitrogen assimilation or growth rate linked to the N status (N : C = NC), which varies between maximum (*NCm*) and minimum (*NCo*) values. FM uses the curvilinear quota function with a half-saturation constant *Kq;* this enables an accurate description of the relationship between N status and growth rate. The form of this function used in recent versions of FM (e.g. Flynn and Hipkin 1999) is given in Eq. 1 (Table 2). This yields a value of *NCu* between 0 and 1, irrespective of the value of *Kq*. In contrast, GM uses the simplified version that assumes a linear function, with no *Kq* (Eq. 2). Either model can readily be altered to employ either form of the quota equation. In

Table 1. List of definitions of variables and parameters used in the equations given in Table 2.

Variable	Definition	Units
AAs	N assimilation rate	g N (g C^{-1}) d^{-1}
alpha	Chl *a*–specific initial slope of the PE curve	μg C m^2 (μmol photons g Chl)$^{-1}$
CAAs	Control of dark N assimilation with constant CAA	Dimensionless
CChls	Control of dark Chl *a* synthesis with constant CChl	Dimensionless
ChlC	Chl *a*:C	g Chl *a* (g C)$^{-1}$
ChlCm	Maximum Chl *a*:C	g Chl *a* (g C)$^{-1}$
ChlNm	Maximum Chl *a*:N	g Chl *a* (g N)$^{-1}$
Cres1	Value of N:C with no reserve C (=NCm)	g N (g C^{-1})
Cres2	Constant for defining rate of dark processes	Dimensionless
Cu	Growth rate	g C (g C^{-1}) d^{-1}
E	Irradiance	μmol photons m^{-2} d^{-1}
f	Quotient adjuster (CAA, CChl, or Nred)	Dimensionless
Kq	Constant for the N:C quota control of growth	g N (g C^{-1})
M	Scalar for adjustment of rate of photoacclimation	Dimensionless
Na	C-specific N assimilation rate	g N (g C^{-1}) d^{-1}
Nam	Maximum C-specific N assimilation rate	g N (g C^{-1}) d^{-1}
NC	N:C	g N (g C^{-1})
NCm	Maximum N:C	g N (g C^{-1})
NCo	Minimum N:C	g N (g C^{-1})
Ncost	Cost of C for assimilation of N	g C (g N^{-1})
NCu	Quotient describing the N:C status	Dimensionless
Nreds	Control of dark NO_3^- reduction with constant Nred	Dimensionless
Pcm	Maximum photosynthetic rate	g C (g C^{-1}) d^{-1}
Pqm	Maximum photosynthesis rate at current N:C status	g C (g C^{-1}) d^{-1}
PS	Photosynthesis rate	g C (g C^{-1}) d^{-1}
S	Scalar for adjustment of N-assimilation or transport	Dimensionless
Um	Maximum growth rate	d^{-1}

all simulations presented here, the values of *NCm* and *NCo* were set at 0.2 and 0.05 (mass ratio of N:C).

In GM, the maximum possible (gross) photosynthetic rate, *Pcm*, is C-specific and set as a constant. (Note that in Geider et al. 1998 this parameter, termed P^c_{max}, is erroneously given as both a constant defining the maximum possible photosynthetic rate in table 3 of that paper and as an auxiliary defining the maximum value of photosynthesis at the current N status indicated by *Q* in table 2 of that paper; the former will be described here as *Pcm* and the latter as *Pqm*.) In FM, the value of *Pqm* is scaled to a constant defining the maximum net photosynthetic rate, i.e., the maximum growth rate (*Um*), such that *Um* may be attained when nitrate is used (the most resource-expensive dissolved inorganic N source).

In both FM and GM, *Pqm* is also scaled by the N:C status, as described by the quota function (Eq. 1 or 2). Thus, at low values of N:C, the maximum photosynthetic rate is depressed. Both models cost the reduction of nitrate indirectly, under the assumption that the generation of reductant via fixed C. Both models have components that describe basal and metabolic-related respiration rates.

N-source assimilation: In quota models, there is no differentiation between nutrient transport and incorporation into biomass; the total process of assimilation is described. In a standard N-controlled quota model, the maximum rate of N assimilation is set as the product of the maximum growth rate and the maximum N:C quota. Control of assimilation is thus passive, with N:C incapable of exceeding *NCm* because N assimilation cannot proceed fast enough to support that state. However, when light-limited conditions are considered, N:C may attain *NCm* not because the growth rate is maximal under N-replete conditions but because the supply of C is inadequate. Both GM and FM use active mechanisms that regulate N assimilation to prevent N:C exceeding *NCm* under such conditions. At steady state, both models have similar dynamics to a standard N-limited quota model (e.g., Flynn et al. 1999).

In Geider et al. (1998), the maximum N-source assimilation rate (*Nam*) was set such that $Nam = Pcm \times NCm$ (see table 3 in Geider et al. 1998), thus following the standard quota formulation. However, there is no a priori reason why *Nam* should be constrained in this fashion. The maximum photosynthesis rate, *Pcm*, exceeds the maximum growth rate because a respiration cost for the assimilation of N (at 2 g C g^{-1}N in Geider et al. 1998) is subtracted. N assimilation is controlled in GM by use of a function that rapidly slows the assimilation rate as N:C approaches *NCm*. The relationship between N:C, potential N assimilation, and N-specific growth rates is shown for the original GM model (as GM1) in Fig. 1A. By addition of a scalar, these relationships may be altered readily, shown as GM3 in Fig. 1A. Within GM, there is no differentiation between ammonium and nitrate assimilations, although an interactive term could be incorporated.

In FM, the processes of N transport and incorporation are handled separately, rather than being combined as assimilation in the standard quota model and as in GM. Transport potential in FM varies with N:C in an attempt to simulate the changes in potential that develop with N stress (Flynn

Table 2. Model equations referred to in the text. The full models are available in Web Appendix 1 at http://www.aslo.org/lo/toc/vol_46/issue_7/1794a1.pdf.

$$NCu = \frac{NC - NCo}{NC - NCo + Kq} \times \frac{NCm - NCo + Kq}{NCm - NCo} \tag{1}$$

$$NCu = \frac{NC - NCo}{NCm - NCo} \tag{2}$$

$$fs = f \times \frac{\left(1 - \frac{NC}{Cres1}\right)^4}{\left(1 - \frac{NC}{Cres1}\right)^4 + Cres2} \tag{3}$$

$$\frac{dChlC}{dt} = ChlNm \times Na \times \left[\frac{PS}{alpha \times ChlC \times E}\right] - ChlC \times Cu \tag{4}$$

$$\frac{dChlC}{dt} = ChlCm \times Um \times M \times NCu\left[1 - \frac{PS}{Pqm}\right] \times \frac{\left(1 - \frac{ChlC}{ChlCm}\right)}{\left(1 - \frac{ChlC}{ChlCm}\right) + 0.05} - ChlC \times [Cu + (1 - NCu)\ Um] \tag{5}$$

$$PS = Pqm \times TanH\left(alpha \times E \times \frac{ChlC}{Pqm}\right) \tag{6}$$

$$\frac{dChlC}{dt} = ChlCm \times Um \times M \times NCu \times CAAs\left[1 - \frac{PS}{Pqm}\right] \frac{\left(1 - \frac{ChlC}{ChlCm}\right)}{\left(1 - \frac{ChlC}{ChlCm}\right) + 0.05} - ChlC \times [Cu + (1 - NCu)Um] \tag{7}$$

$$\frac{dChlC}{dt} = ChlCm \times Um \times M \times NCu \times CAAs\left[\frac{PS}{alpha \times ChlC \times E}\right] \frac{\left(1 - \frac{ChlC}{ChlCm}\right)}{\left(1 - \frac{ChlC}{ChlCm}\right) + 0.05} - ChlC[Cu + (1 - NCu)Um] \tag{8}$$

$$\frac{dChlC}{dt} = ChlNm \times AAs\left[\frac{PS}{alpha \times ChlC \times E}\right] - ChlC \times Cu \tag{9}$$

$$\frac{dChlC}{dt} = ChlCm \times Um \times M \times NCu \times CChls\left[1 - \frac{PS}{Pqm}\right] \frac{\left(1 - \frac{ChlC}{ChlCm}\right)}{\left(1 - \frac{ChlC}{ChlCm}\right) + 0.05} - ChlC[Cu + (1 - NCu)Um] \tag{10}$$

et al. 1997, 1999). Ammonium and nitrate transports may far exceed the balanced growth requirement; surge transports (and the ammonium-nitrate interaction) are regulated via an intermediate pool identified as glutamine (Flynn et al. 1997). The form of the default relationship (given in Flynn 2001) between the potential nitrate transport rate and N:C for FM (as FM1) is shown in Fig. 1B. For the comparison here, it is not so much the shape of the transport/assimilation curves for GM1 and FM1 that is important but rather the point at which these cross the curves for the N-specific growth rate, as shown in Fig. 1. Thus, the level of N:C at which nitrate assimilation/transport is incapable of matching light-saturated growth is much greater for GM1 than for FM1. As with GM, here we have used a scalar to adjust the magnitude of the N-transport potential in FM. The ammonium transport curve (not shown—but see Flynn et al. 1999 for discussion) is higher and often also crosses the N-specific growth rate curve at a higher N:C. When that is so, the growth rate when ammonium is used will exceed that when nitrate is used at light-saturating conditions (consistent with Thompson et al. 1989). The cost of N assimilation in FM for nitrate is 1.71 g C g^{-1}N for reduction to intracellular ammonium, plus 1.5 g C g^{-1}N for the incorporation of that ammonium, or ammonium that has entered directly, into N biomass (see Flynn and Hipkin 1999 for reasoning).

In GM, N assimilation in darkness proceeds at the same rate as in the light until the respiration of C, coupled with the assimilation of N, raises the N:C value to a level at which N assimilation halts (see Fig. 1A). In FM, dark N assimilation (specifically nitrate reduction and amino acid synthesis) is moderated by a sigmoidal function that describes the availability of ''reserve'' C (Eq. 3, Table 2). The

Table 3. Model constants adjusted in the simulations. All but those in boldface type were tuned to optimize the fit of the model to the experimental data. Descriptions of constants and units are given in Table 1. Not all constants are present in all models.

Model Figure	GM1 3A	GM2 3B	FM1 3C	FM2 3D	GM3 4A	GFM 4B	GMFM 4C	FM3 4D
alpha	7.36	8.19	7.13	8.00	7.11	7.56	7.47	7.89
CAA			**1.00**	**1.00**		**1.00**	**1.00**	**1.00**
CChl								0.19
ChlCm			0.073	0.075		0.081		0.070
ChlNm	0.363	0.521			0.390		0.522	
Cres2			0.0100	0.0001		0.0048	0.0051	0.0001
Kq			1.00	0.40		0.11	0.05	0.05
M			2.95	1.10		1.18		2.79
Ncost	**2.0**	**3.2**	**3.2**	**3.2**	**3.2**	**3.2**	**3.2**	**3.2**
Nred			**0.60**	**0.60**		**0.60**	**0.60**	0.86
Pcm	1.72	1.48			2.90			
S	**1.00**	**1.00**	**1.00**	0.95	0.24	1.00	0.98	0.95
Um			1.57	1.54		1.32	1.22	1.26

shape of the curve is defined by the value of the constant Cres2 (default value of 0.01), whereas the quotient is modified by the constant *f*. Thus, for dark amino acid synthesis, *f* and *fs* in Eq. 3 are termed, respectively, *CAA* and *CAAs*, and for dark nitrate reduction, *Nred* and *Nreds*. The default values (set arbitrarily) of constants *CAA* and *Nred* are 1 and 0.6, respectively, so that in darkness nitrate reduction proceeds as 60% of the rate at which amino acid synthesis using internal ammonium may proceed (see Flynn et al. 1997). Other metabolic activities in darkness may be controlled by similar functions.

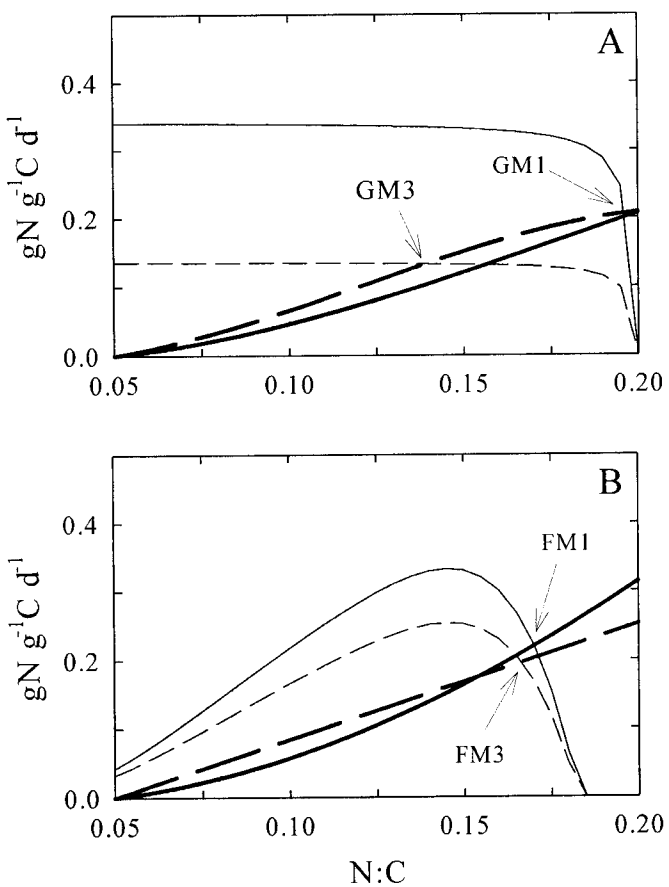

Fig. 1. Relationship between N-specific growth rate (bold lines) and nitrate transport potential (thin lines) for (A) GM1(solid lines) and GM3 (dashed lines), and (B) FM1 (solid lines) and FM3 (dashed lines). The arrows indicate the point at which nitrate transport can only support a higher N : C if C (i.e., light) is limiting.

Photoacclimation: In GM, photoacclimation is modulated by an excitation term that relates the capacity of the light-reactions to demand for photoreductant. The basis of this control is that acclimation in the chlorophyte *Dunaliella* and in higher plants is regulated at least in part by the redox state of the plastoquinone pool (Escoubas et al. 1995; Pfannschmidt et al. 1999). Photoacclimation in FM is related to the level of C supply versus demand. The work of Clark et al. (1999), Clark (2001), and other data from the experiments described in Clark and Flynn (2000) (D.R. Clark unpubl. data) showed that Chl *a* content is enhanced when marine phytoplankton are subjected to dissolved inorganic C stress under conditions where the photon flux density (PFD) is invariant. In GM, synthesis of Chl *a* is a function of concurrent N assimilation (synthesis cannot occur even in N-replete cells without N assimilation), whereas in FM it is a function of current N status (a degradation term is then required to enhance the decline in Chl *a* with a poor N status).

In both models, the photosynthesis rate (PS) is computed via a Jassby and Platt (1976) type of photosynthesis-irradiance (PE) curve, making reference to a constant that describes the Chl-specific initial slope of the PE curve, the current values of Chl : C, and the maximum current photosynthetic rate, *Pqm*. The latter is a similar function of the N : C ratio in both models, and the dynamics of acclimation to N deprivation and N refeeding are thus functions of the N : C component of the respective models (Eq. 1 and 2, Table 2).

The equations that describe synthesis and degradation of Chl *a*, specifically of Chl : C ratio (*ChlC*), are given as Eqs. 4 and 5 (Table 2) for the original GM (GM1) and FM (FM1) configurations. The reasoning behind the construction of the

equations are given in the original papers. The parts of these equations primarily responsible for the control of photoacclimation are within square brackets, with the definition of the PE curve used here as Eq. 6. Alternative formulations for PE curves given by Jassby and Platt (1976), and others may be used as desired.

Modifications to the original models: GM1 was constructed according to Geider et al. (1998), with deletion of the enhanced Chl degradation term (Eq. 4, Table 2). In configurations GM2 and GM3, Eq. 4 was unchanged, but the cost of assimilating nitrate (set at 2 g C g^{-1}N in GM1) was altered to 3.21 (see Flynn and Hipkin 1999); this value of 3.21 was employed for all other models tested here. In addition, in GM3, the value of *Nam*, the maximum rate of N assimilation (originally set as $Pcm \times NCm$) was rescaled by inclusion of a new constant (S) so that $Nam = S \times Pcm \times NCm$. This enables changes to be made affecting the interaction between N-assimilation and N : C (Fig. 1A).

FM1 was constructed according to Flynn and Fasham (1997) with the photoacclimative component from Flynn and Flynn (1998). In the original description by Flynn and Flynn (1998), synthesis of Chl *a* was enabled in darkness, whereas in Flynn and Hipkin (1999), synthesis was disabled. Altering the value of *M* (Eq. 5, Table 2) enables a tuning of the photoacclimative rate with these extremes of synthesis in darkness. For FM2 (as described by Flynn 2001), the rate of Chl *a* synthesis in darkness was modulated by the availability of previously fixed C via the quotient controlling dark amino acid synthesis. Accordingly, Eq. 7 (Table 2) differs from Eq. 5 only in the addition of *CAAs*.

Model GFM differs from FM2 in that the ultimate control of photoacclimation (given within square brackets in the equations) was that used in GM (Eq. 8, cf. Eq. 4 and 7). For model GMFM, the entire photoacclimation system in FM was replaced by one analogous to that in GM. The only difference is that reference is made to the rate of N assimilation at the rate of amino acid synthesis (*AAs*) rather than to N-source uptake as in GM (Eq. 9, cf. Eq. 4). This is necessary within models (such as the ANIM family of models, Flynn et al. 1997) in which transport (into internal pools) of a nutrient may not be concurrent with assimilation into organic N. Finally, model FM3 takes the control of processes in darkness one step further by not only having separate dark-regulation of nitrate reduction and amino acid synthesis but also of Chl *a* synthesis. Hence, in Eq. 10 (Table 2), *CAAs* in Eq. 7 is replaced by *CChls*.

Experimental data—The data used for the comparisons presented here are those of Anning et al. (2000). These describe changes in growth rate, cellular N : C, and Chl : C for the marine diatom *Skeletonema costatum* during transitions in photon flux density (supplied in a 12 h : 12 h light : dark cycle) from 50 μmole photons m^{-2} s^{-1} to 1,200 and back again. The experiment was conducted in cultures supplied with an excess of nitrate. Fig. 2 displays the data for N : C and Chl : C (replicate data from two experiments). There is significant ''noise'' within the latter part of the N : C series (days 10–15 after the down-light shock to 50 μmole photons m^{-2} s^{-1}). The source of the noise is not clear; it may be associated with experimental factors or perhaps with physiological changes associated with down-light shock.

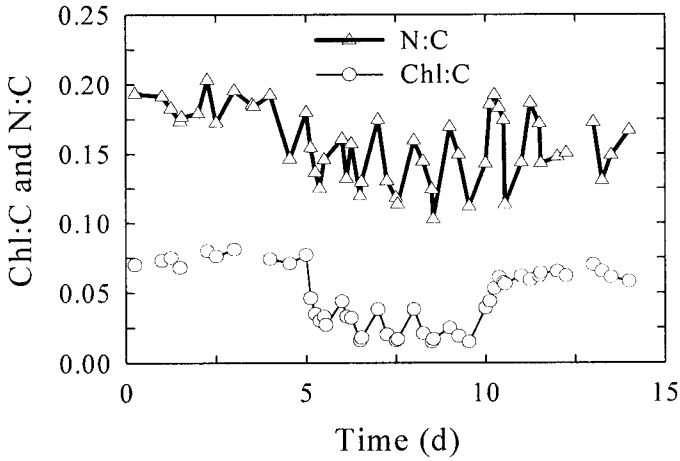

Fig. 2. Data from Anning et al. (2000) for the mass ratios of N : C and Chl *a* : C. Data are joined when the time period between them was ≤0.5 d. The first half of each day was illuminated at 50 μmole photons m^{-2} s^{-1} until day 5 and after day 10 and at 1,200 μmole photons m^{-2} s^{-1} between days 5 and 10. The latter half of each day was in darkness.

Chl : C undergoes a pronounced diel cycle during growth at the high light level (days 5–10), concurrent with a more obvious diel cycle in N : C. Changes in Chl : C and N : C are coupled because Chl : C can change in darkness as a result of Chl *a* synthesis and also C consumption, much of which may be associated with N assimilation in the absence of concurrent photosynthesis (which will also act to elevate N : C). An analysis of the raw experimental data for C, N, and Chl (all as g ml^{-1} of culture) showed no significant changes in these concentrations during the dark period in the low-light cultures. However, on average, C declined by 17%, whereas Chl *a* increased by 68% and N increased by 24% in the high-light incubation period (the period between days 5 and 10 in Fig. 2). Given the average values for changes over the dark period of the high light incubations, a typical Chl : C of 0.017 at the end of the light period had increased to 0.033 by the start of the following light period. Concurrently, a typical N : C of 0.117 increased to 0.175.

Simulations—The models were tuned to the data with light either supplied as in reality, within a square-wave light : dark cycle, or continuously with the appropriate 24-h photon dose (the latter approach is more common in ecosystem models). Model configurations were tuned by use of common constants for these two light scenarios. Because both GM and FM models employ scalars for, respectively, gross (*Pcm*) or net (*Um*) photosynthesis, these rates need to be doubled when operating under a 12 h : 12 h light : dark cycle. The models all assumed the same maximum and minimum N : C (0.2 and 0.05, respectively). Tuning of constants was undertaken by use of a genetic algorithm as supported by Powersim Solver v2. The values of constants used in the simulations are given in Table 3.

Table 4. Goodness of fit comparison between the model output and steady-state experimental data at the two contrasting light levels, for growth rate (μ), Chl : C and N : C, as judged by fitting a linear regression. Time plots for Chl : C and N : C are given in the figures indicated. Where possible, regressions were forced through (0,0). An optimal fit would achieve slope and r^2 values of 1.0, with a constant of 0. The models were run either with light supplied continuously as a 24-h dose of photons (cl) or in a 12:12 h light : dark cycle (ld).

			μ			Chl : C			N : C		
Model	Figure	Light	Slope	Const.	r^2	Slope	Const.	r^2	Slope	Const.	r^2
GM1	3A	cl	1.07	0	0.96	0.80	0	0.66	0.04	0.19	0.34
		ld	1.07	0	0.96	0.81	0	0.79	0.03	0.19	0.20
GM2	3B	cl	0.36	0.46	1.00	0.97	0	0.62	0.02	0.20	0.30
		ld	0.36	0.46	1.00	1.00	0	0.78	0.02	0.20	0.13
FM1	3C	cl	1.05	0	0.98	0.95	0	0.81	0.22	0.12	0.35
		ld	0.94	0	0.99	0.85	0	0.74	0.37	0.09	0.32
FM2	3D	cl	1.03	0	0.99	0.79	0	0.78	0.10	0.16	0.35
		ld	0.96	0	099	1.01	0	0.71	0.45	0.10	0.31
GM3	4A	cl	0.96	0	0.81	0.88	0	0.82	0.59	0.07	0.28
		ld	1.06	0	0.98	099	0	0.87	0.61	0.08	0.34
GFM	4B	cl	1.06	0	1.00	0.87	0	0.75	0.05	0.16	0.32
		ld	0.96	0	0.90	1.10	0	0.80	0.43	0.09	0.37
GMFM	4C	cl	1.08	0	0.95	0.93	0	0.67	0.06	0.15	0.30
		ld	0.97	0	0.91	1.02	0	0.89	0.57	0.06	0.44
FM3	4D	cl	1.03	0	0.98	0.84	0	0.77	0.16	0.15	0.37
		ld	0.98	0	0.98	0.98	0	0.91	0.69	0.05	0.40

Results—GM1 uses the original configuration of Geider et al. (1998). The model reports the correct growth rates (Table 4), but N : C is flat and too high (Fig. 3A). Although the fit to Chl : C is reasonable (Table 4), the rate of acclimation to the low light shift (days 10–15 in Fig. 3A) is too slow.

GM2 is the same as GM1 except in the use of a more realistic cost for the assimilation of N (*Ncost*, Table 3). The fit to Chl : C (Table 4, Fig. 3B) is now improved, especially the rate of acclimation after day 10 (Fig. 3B), but N : C is no different. Furthermore, the model is no longer capable of reproducing the growth rates correctly (Table 4). This is because the fitted value of the maximum carbon-specific photosynthesis rate (*Pcm*) is lower in GM2 than in GM1 (Table

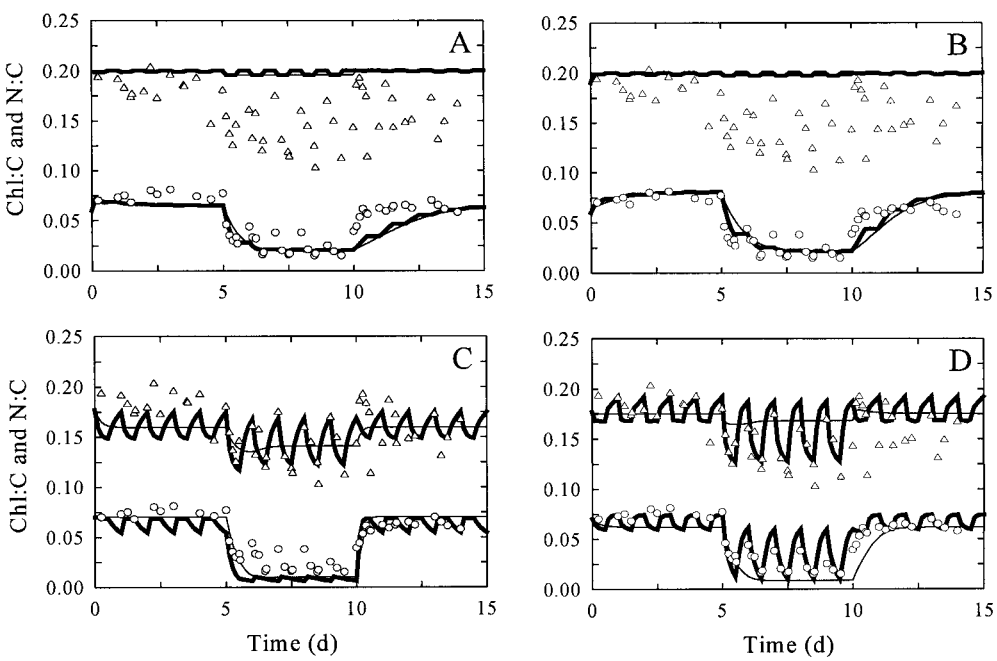

Fig. 3. Comparisons of model output with experimental data for N : C (triangles) and Chl : C (circles); cf. Fig. 2. Panels present model output from (A) GM1, (B) GM2, (C) FM1, and (D) FM2. Thin lines are for simulations where light was supplied continuously to attain the daily photon dose. Thick lines are for simulations where light was supplied in a 12 h : 12 h light : dark cycle, as used in the experiments.

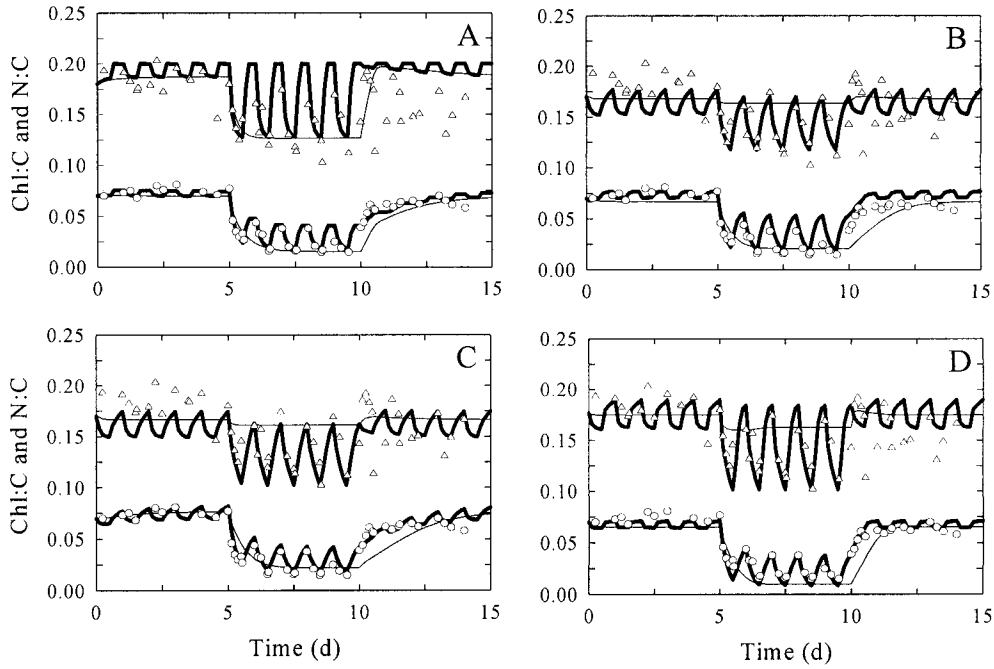

Fig. 4. As Fig. 3, except that panels present model output from (A) GM3, (B) GFM, (C) GMFM, and (D) FM3.

3), and the disparity between the potential for N assimilation and N-specific growth already present in GM1 (see Fig. 1A) is exacerbated in GM2 by the use of a higher (more realistic) respiration value (Table 3).

The original version of FM, with synthesis of Chl *a* enabled in darkness, showed an extreme, unacceptable, diel oscillation in Chl : C during the high-light period (not shown). This was because the value of Chl : C attained the same level as that in the low-light period by the end of each dark phase. (This problem does not affect the work of Flynn and Flynn 1998, because that study was directed toward low light and N colimitation.) The behavior of the same model, FM1, but with synthesis disabled in darkness (as used in Flynn and Hipkin 1999) fails to simulate the pronounced diel oscillation of Chl : C in the high-light phase (days 5–10 in Fig. 3C), although the fit to the data is acceptable (Table 4). FM1 also gives a good fit to the growth rate (Table 4) and a N : C oscillation that is greater during the high-light period (Fig. 3C), as expected (Fig. 2).

Model FM2 (as in Flynn 2001) shows a considerable improvement over FM1 for the simulation of Chl : C (Table 4, Fig. 3D), with the dark synthesis of Chl : C now linked to the availability of C reserves generated during the previous light phase. However, the fit to N : C is no better, and the fit to Chl : C in the continuous illumination simulation is too low during the high-light period (days 5–10).

Turning now to new modifications of the models, GM3 introduces a scalar to adjust the N-assimilation capacity in comparison with the gross C-fixation rate (*Pcm*) and its accompanying N-specific growth rate (Fig. 1A). The tuned value of *Pcm* is now almost double that for GM1 (Table 3). The fit of this configuration is excellent for growth rate (Table 4) and Chl : C (Fig. 4A), including the rate of acclimation. The N : C also shows a cyclic variation in keeping with the data (Fig. 4A).

Placement of the GM photoacclimation component within FM2, giving GFM (Fig. 4B), gives a similar output to that from FM2 (Table 4), except that the fit of Chl : C during the high-light period is improved. In model GMFM, the entire Chl *a* synthesis component of FM is replaced by its GM counterpart. This (Fig. 4C, Table 4) provides a further slight improvement over FM2 and GFM, with only the slow rate of acclimation to low light (days 10–15) in the continuous light simulation being of concern.

Finally, FM3 (Fig. 4D) includes the capability to control N assimilation and Chl *a* synthesis in darkness separately. This gives the best fits of all the models to the data (Table 4), with the exception of N : C in the continuous light simulation.

Discussion—None of these models (except for FM1 with dark Chl : C synthesis enabled) produce unsatisfactory simulations of the Chl : C data of Anning et al. (2000). However, taken overall (considering growth rate, N : C, and Chl : C), configurations GM1, GM2, and FM1 have significant shortcomings (Fig. 3, Table 4). FM1 with dark Chl : C synthesis disabled also fails to reproduce the expected diel changes in Chl : C (Fig. 3C), even though the proportion of variability accounted for by the model is acceptable (Table 4).

The problems in the original GM (GM1 and GM2) are within the N-assimilation component of the model, specifically in the choice of the value of the maximum N-assimilation rate (*Nam*) relative to the maximum photosynthetic rate (*Pcm*). Because of the simple form of control of N assimilation with N : C (Fig. 1A), under N-replete conditions N : C will always be close to *NCm* (Fig. 3A and B), unless

Pcm is significantly greater than *Nam*/*NCm*. Model output is much improved (Fig. 4A) when the N-assimilation capability is rescaled and the fitted maximum gross photosynthetic rate is increased (GM3 in Fig. 1A and Table 3). This model, GM3, also used a more realistic cost for N-assimilation.

In contrast, the problems in FM1 lie within the photoacclimative component of the model, specifically in the control of Chl synthesis in darkness. In GM, Chl synthesis is scaled to the rate of N assimilation and will thus continue only if there is sufficient C to support N assimilation in darkness. However, in FM1, synthesis is scaled directly to the whole organism N : C such that, if that is high, then Chl synthesis is also high. Although disabling synthesis in darkness gives an adequate output (FM1, Table 4), it is clearly seen in the original data that Chl *a* synthesis does indeed proceed in darkness. The error is corrected in FM2 by using the existing quotient within ANIM models (Flynn et al. 1997) that controls dark amino acid synthesis to also control Chl synthesis.

The problems identified above in the original models were not seen in the hybrid constructions. The combinations of GM and FM, GFM (Fig. 4B), and GMFM (Fig. 4C) were both successful because they combined the N-assimilation component of FM with the photoacclimative components of GM. Model FM3 provides a further level of control with a separate regulation of dark synthesis of Chl : C. Although diatoms, such as *S. costatum*, may continue to assimilate nitrate at high rates in darkness (given sufficient reserve C), many other algae cannot do so. Dinoflagellates in particular are poor at dark nitrate assimilation while being able to use ammonium (Flynn and Flynn 1998). The suitability of the GM structure, which couples N assimilation and Chl : C synthesis, for simulating different species when assimilating different N sources needs to be examined. The structure of FM3 provides greater flexibility for handling different behavioural responses.

As total model constructs, the GM structure is considerably smaller, lacking the internal pool components of the ANIM family of models (Flynn et al. 1997; Flynn and Fasham 1997). Where one wishes to simulate only the interaction between a single N source and light, it is most logical to consider the use of GM (as modified in GM3) first. For more complex scenarios, such as ammonium-nitrate interactions and N assimilation in darkness, FM is more appropriate, because it contains more detail of physiological processes. GMFM was used as the basis for the photoinhibition model of Marshall et al. (2000) for this reason.

Whether one wishes to use the revised FM (Eqs. 7 or 10) or GM (Eq. 9) photoacclimation component within ANIM-family models (which now includes a single structure for ammonium-nitrate-P-Si-Fe-light-temperature interactions; Flynn 2001) is largely a matter of personal preference. However, the GM component consistently gives a better simulation of Chl : C within continuous light conditions for the high-light period (Figs. 3, 4), with the FM approach giving values that are too low. This can be seen most clearly between FM2 (Fig. 3D) in comparison with GFM (Fig. 4B) and GMFM (Fig. 4C). The driving force behind photoacclimation in these models when operating in a continuous light dose scenario at high irradiance thus appears to be better simulated by use of the excitation term in GM (within square brackets in Eq. 4, Table 2) than the C-demand term in FM (within square brackets in Eq. 5).

Kevin J. Flynn[1] *and Helen Marshall*

Ecology Research Unit
University of Wales Swansea
Swansea SA2 8PP, Wales, UK

Richard J. Geider

Department of Biological Sciences
University of Essex
Colchester, CO4 3SQ, England, UK

References

ANNING, T., H. L. MACINTYRE, S. M. PRATT, P. J. SAMMES, S. GIBB, AND R. J. GEIDER. 2000. Photoacclimation in the marine diatom *Skeletonema costatum.* Limnol. Oceanogr. **45:** 1807–1817.

CLARK, D. R. 2001. Carbon and nitrogen co-limitations in the diatom *Thalassiosira.* J. Phycol. **37:** 249–256.

———, AND K. J. FLYNN. 2000. The relationship between the dissolved inorganic carbon concentration and growth rate in marine phytoplankton. Proc. R. Soc. Lond. B. **267:** 953–959.

———, M. J. MERRETT, AND K. J. FLYNN. 1999. Utilization of dissolved inorganic carbon (DIC) and the response of the marine flagellate *Isochrysis galbana* to carbon or nitrogen stress. New Phytol. **144:** 463–470.

ESCOUBAS J., M. LOMAS, J. LAROCHE, AND P. FALKOWSKI. 1995. Light intensity regulation of *cab* gene transcription is signaled by the redox state of the plastoquinone pool. Proc. Natl. Acad. Sci. USA **92:** 10237–10241.

FLYNN, K. J. 1999. Nitrate transport and ammonium-nitrate interactions at high nitrate concentration and low temperature. Mar. Ecol. Prog. Ser. **189:** 283–287.

———. 2001. A mechanistic model for describing dynamic multinutrient, light, temperature interactions in phytoplankton. J. Plankton Res. **23:** 977–997.

———, AND M. J. R. FASHAM. 1997. A short version of the ammonium-nitrate interaction model. J. Plankton Res. **19:** 1881–1897.

———, M. J. R. FASHAM, AND C. R. HIPKIN. 1997. Modelling the interaction between ammonium and nitrate uptake in marine phytoplankton. Phil. Trans. R. Soc. Lond. **352:** 1625–1645.

———, AND K. FLYNN. 1998. The release of nitrite by marine dinoflagellates—development of a mathematical simulation. Mar. Biol. **130:** 455–470.

———, AND C. R. HIPKIN. 1999. Interactions between iron, light, ammonium, and nitrate: Insights from the construction of a dynamic model of algal physiology. J. Phycol. **34:** 1171–1190.

———, S. PAGE, G. WOOD, AND C. R. HIPKIN. 1999. Variations in the maximum transport rates for ammonium and nitrate in the prymnesiophyte *Emiliania huxleyi* and the raphidophyte *Heterosigma carterae.* J. Plankton Res. **21:** 355–371.

GEIDER, R. J., H. L. MACINTYRE, AND T. M. KANA. 1996. A dynamic model of photoadaptation in phytoplankton. Limnol. Oceanogr. **41:** 1–15.

[1] Corresponding author (k.j.flynn@swansea.ac.uk).

Acknowledgements

This work was supported by the Natural Environment Research Council of the UK through grants to K.J.F. and R.G. and a studentship to H.M.

———, ———, AND ———. 1997 A dynamic model of phytoplankton growth and acclimation: Responses of the balanced growth rate and chlorophyll *a:* Carbon ratio to light, nutrient-limitation and temperature. Mar. Ecol. Prog. Ser. **148:** 187–200.

———, ———, AND ———. 1998. A dynamic regulatory model of phytoplanktonic acclimation to light, nutrients, and temperature. Limnol. Oceanogr. **43:** 679–694.

JASSBY, A. D., AND T. PLATT. 1976. Mathematical formulation of the relationships between photosynthesis and light for phytoplankton. Limnol. Oceanogr. **21:** 540–547.

MARSHALL, H. L., R. J. GEIDER, AND K. J. FLYNN. 2000. A mechanistic model of photoinhibition. New Phytol. **145:** 347–359.

PFANNSCHMIDT, T., A. NILSSON, AND J. F. ALLEN. 1999. Photosynthetic control of chloroplast gene expression. Nature **397:** 625–628.

THOMPSON, P. A., M. E. LEVESSAUR, AND P. J. HARRISON. 1989. Light-limited growth on ammonium vs nitrate: What is the advantage for marine phytoplankton? Limnol. Oceanogr. **34:** 1014–1024.

ZONNEVELD, C. 1998*a*. Light-limited microalgal growth: A comparison of modelling approaches. Ecol. Model. **113:** 41–54.

———. 1998*b*. A cell-based model for the chlorophyll *a* to carbon ratio in phytoplankton. Ecol. Model. **113:** 55–70.

Received: 27 April 2001
Amended: 29 June 2001
Accepted: 18 July 2001

Limnol. Oceanogr., 46(7), 2001, 1802–1808

Iron uptake and physiological response of phytoplankton during a mesoscale Southern Ocean iron enrichment

Abstract—Iron supply is thought to regulate primary production in high nitrate, low chlorophyll (HNLC) regions of the sea in both the past and the present. A critical aspect of this relationship is acquisition of iron (Fe) by phytoplankton, which occurs through a complex series of extracellular reactions that are influenced by Fe chemistry and speciation. During the first in situ mesoscale Fe-enrichment experiment in the Southern Ocean (Southern Ocean iron release experiment [SOIREE]), we monitored the uptake of Fe by three size classes of plankton and their ensuing physiological response to the Fe enrichment. Rates of Fe uptake from both inorganic Fe (Fe′) and organic Fe complexes (FeL) were initially fast, indicative of Fe-limitation. After Fe enrichment phytoplankton down-regulated Fe uptake and optimized physiological performance, but by day 12 they had greatly increased their capacity to acquire Fe from FeL. The increase in Fe uptake from FeL coincided with a sixfold decrease in Fe′ that followed the production of Fe-binding organic ligands. Phytoplankton were able to use organically bound Fe at rates sufficient to maintain net growth for more than 42 d. Adaptation to such shifts in Fe chemistry may contribute to bloom longevity in these polar HNLC waters.

High nitrate, low chlorophyll (HNLC) waters account for 25% of the world surface ocean and have been the focus of recent investigations examining what factor(s) control primary productivity. Culture (Sunda and Huntsman 1997) and shipboard (Martin et al. 1989; Coale et al. 1996*a*) studies show that low Fe availability limits phytoplankton growth, a result that has been confirmed by in situ Fe enrichments in HNLC regions (Martin et al. 1994; Coale et al. 1996*b;* Boyd et al. 2000). The chemical complexities of Fe and its potential interactions with microbes in natural waters, however, may obfuscate the relationship between phytoplankton physiology and Fe concentrations (Geider 1999). Physiological adaptations of Fe-limited phytoplankton include variations in inorganic Fe uptake kinetics (Harrison and Morel 1986; Hudson and Morel 1990) and in their abilities to acquire Fe from organic Fe complexes (FeL) (Maldonado and Price 1999, 2001). However, the physiological responses of natural phytoplankton assemblages to shifts in Fe speciation in situ are unknown. Pronounced in situ changes in Fe speciation occurred during IronEx II in the Equatorial Pacific (Rue and Bruland 1997), but no concurrent measurements of algal Fe uptake physiology were made. Because Fe speciation strongly affects the ability of phytoplankton to acquire Fe (Geider 1999; Maldonado and Price 1999, 2001), changes in Fe speciation will undoubtedly determine the algal response to Fe enrichment.

Southern Ocean waters are characterized by a large reservoir of macronutrients and are thought to have a disproportionate influence on past and present global climate (Broecker and Henderson 1998; Sarmiento et al. 1998). The SOIREE (Boyd et al. 2000) was conducted in February 1999 to assess whether Fe supply controls phytoplankton production in polar waters (61°S 140°E). A 50 km^2 area of surface ocean was fertilized with inorganic Fe(II) labeled with SF_6 (sulfur hexafluoride) and with three subsequent additions of Fe on days 3, 5, and 7 of the experiment (Fig. 1A) (Boyd et al. 2000). The Fe enrichment resulted in significant changes in Fe speciation and dissolved Fe concentrations. Within 13 d, a pronounced accumulation of phytoplankton stocks, an increase in growth rate and photosynthetic competence of the dominant taxa, and a change in species composition were observed (Boyd et al. 2000). Moreover, SeaWiFS remote-sensing images of the Fe-fertilized patch showed that the bloom was still present 42 d after the onset of SOIREE and had spread over a ribbon-shaped area of 1,100 km^2 (Abraham et al. 2000). This observation raised fundamental questions regarding the mechanisms for the sustenance and longevity of this bloom. This paper investigates the physiological response of plankton to changes in Fe chemistry and speciation following this in situ Fe enrichment